Translational Oncology
www.transonc.com

Volume 12 Number 9 September 2019 pp. 1155–1163 1155

High Glucose Promotes Human Glioblastoma Cell Growth by Increasing the Expression and Function of Chemoattractant and Growth Factor Receptors[1]

Zhiyao Bao[*,†,2], Keqiang Chen[†,2], Stacey Krepel[†], Peng Tang[†,‡], Wanghua Gong[§], Meihua Zhang[¶,†], Weiwei Liang[#,†], Anna Trivett[†], Min Zhou[*] and Ji Ming Wang[†]

[*]Department of Pulmonary and Critical Care Medicine, Shanghai Institute of Respiratory Disease, Ruijin Hospital Affiliated to Shanghai Jiao Tong University School of Medicine, Shanghai 200025, PR China; [†]Cancer and Inflammation Program, Center for Cancer Research, National Cancer Institute at Frederick, MD 21702, USA; [‡]Department of Breast Surgery, Southwest Hospital, Third Military Medical University, Chongqing 400038, China; [§]Basic Research Program, Leidos Biomedical Research, Inc., Frederick, MD 21702, USA; [¶]Maternal and Child Health Care Hospital of Shandong Province, Jinan, Shandong 250002, China; [#]Department of Immunology, School of Basic Medical Sciences, and Key Laboratory of Medical Immunology of Ministry of Health, Peking University Health Science Center, Beijing 100191, China

Abstract

Diabetes mellitus, characterized by hyperglycemia, is considered as a risk factor of cancers including malignant gliomas. However, the direct effect of high glucose on cancer cell behavior is not clear. We therefore investigated the effect of hyperglycemia on the growth of human glioblastoma (GBM) cells. Our results revealed that high glucose (HG) promoted the proliferation and inhibited the apoptosis of a human GBM cell line U87. Mechanistically, HG upregulated the expression and function of a G-protein coupled chemoattractant receptor (GPCR) formyl peptide receptor 1 (FPR1) and epidermal growth factor receptor (EGFR) on GBM cells, which upon activation by their agonists, promoted cell migration and proliferation. In addition, the invasiveness and the production of VEGF by U87 cells were enhanced under HG conditions, the effects of which were mediated by FPR1 and EGFR agonists. The tumor promoting activity of HG was further substantiated by increased tumorigenicity and growth of xenograft tumors formed by GBM cells in nude mice with induced diabetes mellitus. Thus, our study demonstrates the capacity of HG to promote GBM progression via enhancement of the function of chemoattractant and growth factor receptors.

Translational Oncology (2019) 12, 1155–1163

Address all correspondence to: Ji Ming Wang, Center for Cancer Research, National Cancer Institute, Bldg. 560 Rm 31-68, Frederick MD 21702-1201. or Min Zhou, Department of Pulmonary and Critical Care Medicine, Shanghai Institute of Respiratory Disease, Ruijin Hospital Affiliated to Shanghai Jiao Tong University School of Medicine, Shanghai 200025, P. R. China E-mail: doctor_zhou_99@163.com

[1] Grant Support: This project has been funded in part by Federal funds from the National Cancer Institute (NCI), National Institutes of Health (NIH), under Contract No. HSN261200800001E, and is also supported in part by the Intramural Research Program of NCI, NIH. Zhiyao Bao was also supported in part by grant No. 81600004 from the National Nature Science Foundation of China and grant No. YG2016QN63 from Shanghai Jiaotong University.

[2] These authors contributed equally to this study.

Received 8 March 2019; Revised 19 April 2019; Accepted 22 April 2019

1936-5233/19
https://doi.org/10.1016/j.tranon.2019.04.016

Introduction

Glioblastoma (GBM) is the most common and aggressive subtype of gliomas with poor patient survival despite the treatment [1]. Putative risk factors for gliomas include aging, male gender and white ethnicity, without effective means of prevention [2]. Studies suggest that elevated blood glucose is associated with increased malignancy and the rate of recurrence of gliomas [3,4]. Hyperglycemia is a hallmark for diabetes mellitus (DM), which is the most common endocrine disorder [5]. Patients with DM experience higher incidence of cancers [6], including cancers of the liver, pancreas, endometrium, colon/rectum and breast [7]. High glucose (HG) triggers intracellular pathways, which promote cancer progression, such as increased leptin levels and pro-cell survival AKT/mTOR, enhancement of WNT/β-catenin signaling, induction of epithelial mesenchymal transition, and upregulation of inflammatory cytokine levels in circulation [4,6–8]. However, the effect of HG on GBM cell behavior is not clear.

Our previous study showed that in Müller glial cells (MGC) of the retina, HG enhanced the functional expression of a G protein-coupled formylpeptide receptor 2 (FPR2), originally found to mediate leukocyte migration in response to bacterial and endogenous chemotactic peptides. In MGCs, HG enhances cell migration, proliferation and the production of vascular endothelial growth factor (VEGF) via FPR2 to exacerbate diabetic retinopathy [9]. Human GBM cells express an FPR2 variant, FPR1, which is stimulated by necrotic tumor cell-released agonist to promote cell chemotaxis, survival, and tumorigenesis in xenograft models [10,11]. In human GBM specimens, FPR1 is preferentially expressed by higher grade tumors, which is associated with poorer patient survival [10]. These observations prompted us to investigate the contribution of HG to the malignant behavior of human GBM cells and the underlying mechanisms. Here, we report that human GMB cells in HG express increased levels of FPR1 as well as the receptor for EGF (EGFR), in association with more rapid tumor progression in diabetic animals.

Materials and Methods

Reagents

The source of reagents is detailed in Supplemental Materials.

Cell Lines and Culture

Human GBM cell line U87 was obtained from American Type Culture Collection (Manassas, VA) and grown in Dulbecco's modified Eagle medium (DMEM) containing 10% FCS and 1% penicillin–streptomycin. Rat basophil leukemia cell line transfected with FPR1 gene (ETFR cells) was a gift from Dr. R. Snyderman (Duke University,

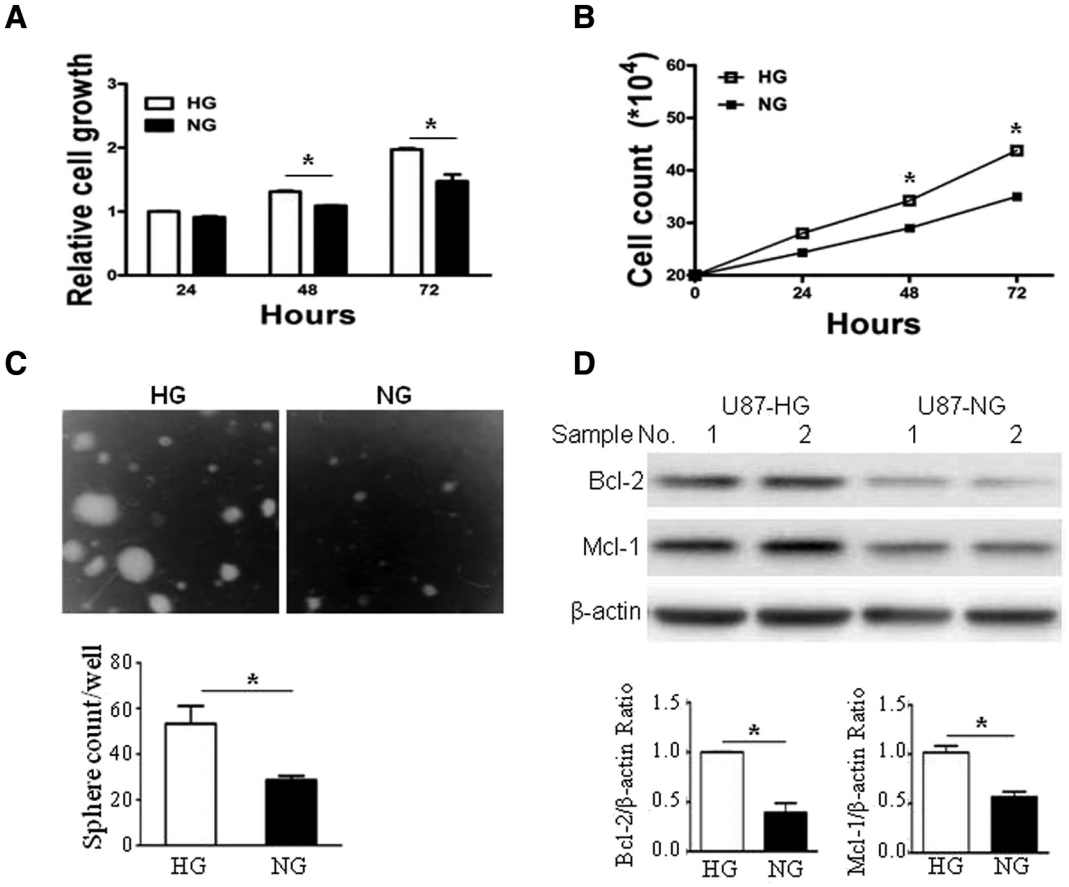

Figure 1. High glucose promotes U87 cell proliferation and survival U87 cells were exposed to high (25.0 mM, HG) or normal glucose (5 mM, NG) for 24, 48 and 72 h. **A.** Cell proliferation assessed by MTT assay. **B.** Cells were counted using inverted microscopy. **C.** The effect of glucose on long term growth of U87 cells assessed through microsphere formation. Graphs represent the mean ± SEM of triplicate samples (n = 3). *$P < .05$, indicates significantly increased growth and sphere formation of U87 cells under HG compared with cells in NG. **D.** U87 cells cultured for 24 h in HG or NG were measured for Bcl-2 and Mcl-1 proteins by Western blotting. Densitometric analyses were shown in lower panel. *$P < .05$, indicates significantly increased Bcl-2 and Mcl-1 in U87 cells in HG culture compared with NG.

Durham, NC) and was grown in DMEM containing 10% FCS, 1% penicillin–streptomycin and G418 (Invitrogen) at 0.8 mg/mL. To study the effect of high glucose, GBM cells were exposed to either normal (physiological) glucose (NG) (5.5 mM) or high glucose (HG) (25.0 mM) concentration in media for indicated time points.

Animals

Male Athymic Ncr-nu/nu mice (4–6 weeks-old, Charles River Laboratories Inc., Frederick, MD) were intraperitoneally injected for five consecutive days of streptozotocin (STZ; 40 mg/kg body wt/day) (Sigma-Aldrich) followed 2 days later by a second round of 5 days consecutive injection to induce diabetes. Mice with stable blood glucose levels above 200 mg/dl are considered diabetic. Animal study was conducted with the approval by Animal Care and Use Committee of the National Cancer Institute at Frederick, NIH.

Tumor Cell Proliferation and Microsphere Formation

The assays for tumor cell proliferation and microsphere formation are detailed in Supplemental Materials.

Western Blotting

Examination of cellular signaling via FPR1 and EGFR under HG or NG is detailed in Supplemental Materials.

RT-PCR

Total RNA was extracted from U87 cells with an RNeasy mini kit and depleted of contaminating DNA with RNase-free DNase (QIAGEN). RT-PCR was performed using the Verso 1-step RT-PCR ReddyMix Kit (Thermo) and 100 ng total RNA. The information of primers and procedures are detailed in Supplemental Materials.

Cell Migration (Chemotaxis)

Chemotaxis assays for U87 cells were performed in 48-well chemotaxis chambers as described previously [12]. For inhibition of chemotaxis, U87 cell cultures in HG or NG were pretreated with the FPR1 antagonist BOC-MLF or the EGFR inhibitor AG1478 for 30 min before placement into chemotaxis chambers.

Cell Monolayer Scratching Wound Healing Assays

Wound-healing assays for U87 cells were performed according to published procedures [13]. For inhibition of wound-healing, U87 cells cultured in HG or NG were pretreated with the FPR1 antagonist BOC-MLF or the EGFR inhibitor AG1478 for 30 min before measurement. Scratches were photographed and the distance of cell migration towards the center of the wound was measured at three positions by Image J software (NIH) (Supplemental Materials).

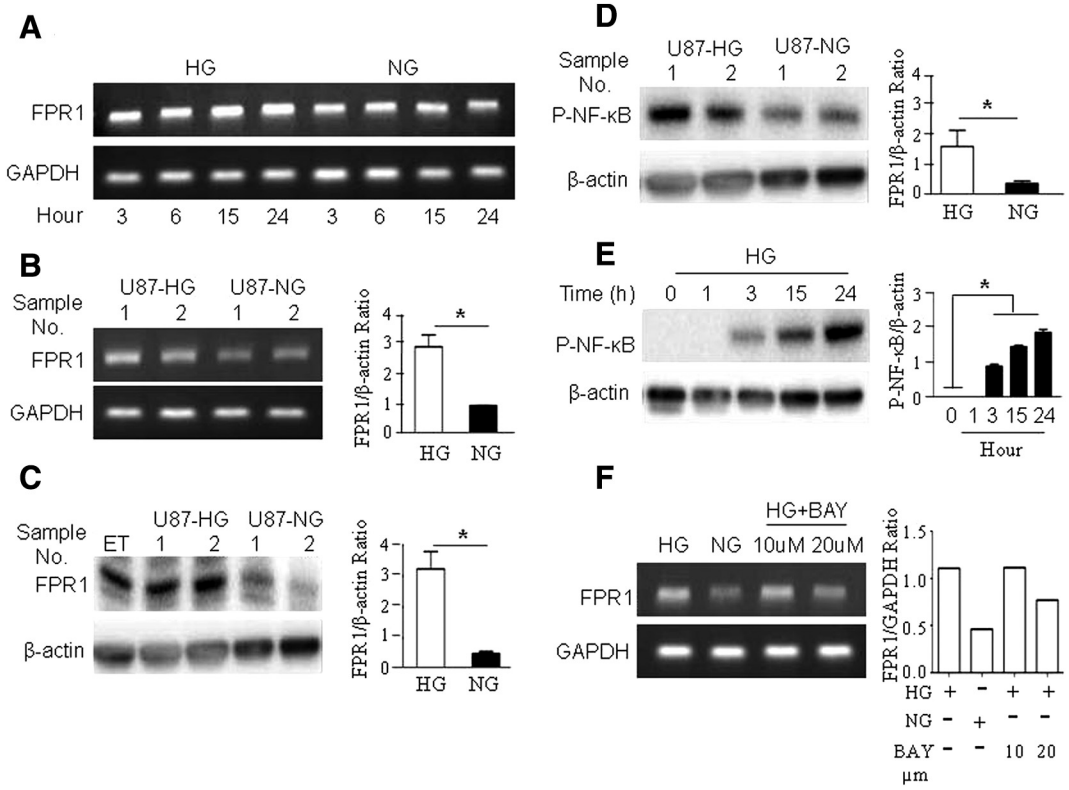

Figure 2. HG up-regulates the expression of FPR1 by U87 cells. U87 cells were cultured in HG or NG for the indicated times. FPR1 mRNA was detected by RT-PCR. **A.** Increased FPR1 mRNA in U87-HG cells. **B.** Higher FPR1 mRNA levels in U87 cells cultured in HG for 24 h. *$P < .05$, indicates significantly increased FPR1 mRNA expression in U87 cells in HG compared with cells in NG culture. **C.** Increased FPR1 protein level in U87-HG measured by Western blotting. Epitope-tagged human FPR transfected RBL (ETFR) cells were cultured in HG for 24 h as positive controls. *$P < .05$, indicates significantly increased FPR1 protein expression in U87 cells in HG compared with cells in NG culture. **D.** Increased NF-κB phosphorylation in U87-HG for 24 h shown by Western blotting. *$P < .05$, indicates significantly increased p-NF-kB in U87 cells in HG compared with cells in NG culture. **E.** Western blotting showing phosphorylation of NF-κB in HG cultured U87 cells at indicated time points. *$P < .05$. **F.** The expression of FPR1 mRNA detected by RT-PCR in U87 cells in HG culture for 24 h are treated with the NF-kB inhibitor BAY 11–7082 at indicated concentrations for 30 min.

Enzyme-Linked Immunosorbent Assay

Confluent U87 cells were cultured in NG or HG media with the absence or presence of fMLF (10^{-7} M) or EGF (10 ng/ml). The supernatants were then collected at 24 h for analysis of VEGF-A with an ELISA kit (Invitrogen, ThermoFisher).

Xenografts

U87 cells (5×10^6 in 200 μl PBS) were implanted s.c. into the flank of diabetic or normal nude mice (as controls). The weight of mice and the tumor size were monitored twice a week. Tumor size was calculated by the formula $lw^2/2$, where l is the length of the tumor in millimeters and w is the width in millimeters. Each group contains at least five mice (See also Supplemental Materials).

Histology and Immunofluorescence for Xenograft Tumors

Freshly frozen, optimal cutting temperature (OCT) compound-embedded xenograft tumors formed by U87 cells were sectioned as 5 μm slides and fixed in 4% neutral buffered formalin for 10 min for hematoxylin and eosin (H&E) staining. Tumor tissues sectioned at 10 μm were used for immunofluorescence staining of Ki67, GFAP, Vimentin and CD31 as detailed in Supplemental Materials. Tissue sections were photographed by using a fluorescence microscope (Olympus BX60). The intensity of fluorescence was analyzed with cellSens Standard software.

Analysis of Microvessel Density (MVD)

MVD was assessed with anti-mouse CD31 immunostaining to define blood vessels. Images were taken at 200× magnification to count CD31 positive cells or cell clusters in three different areas. Final results of MVD were calculated by Image J software (NIH).

Statistical Analysis

All experiments were performed at least 3 times with representative and reproducible results shown. Statistical significance was analyzed

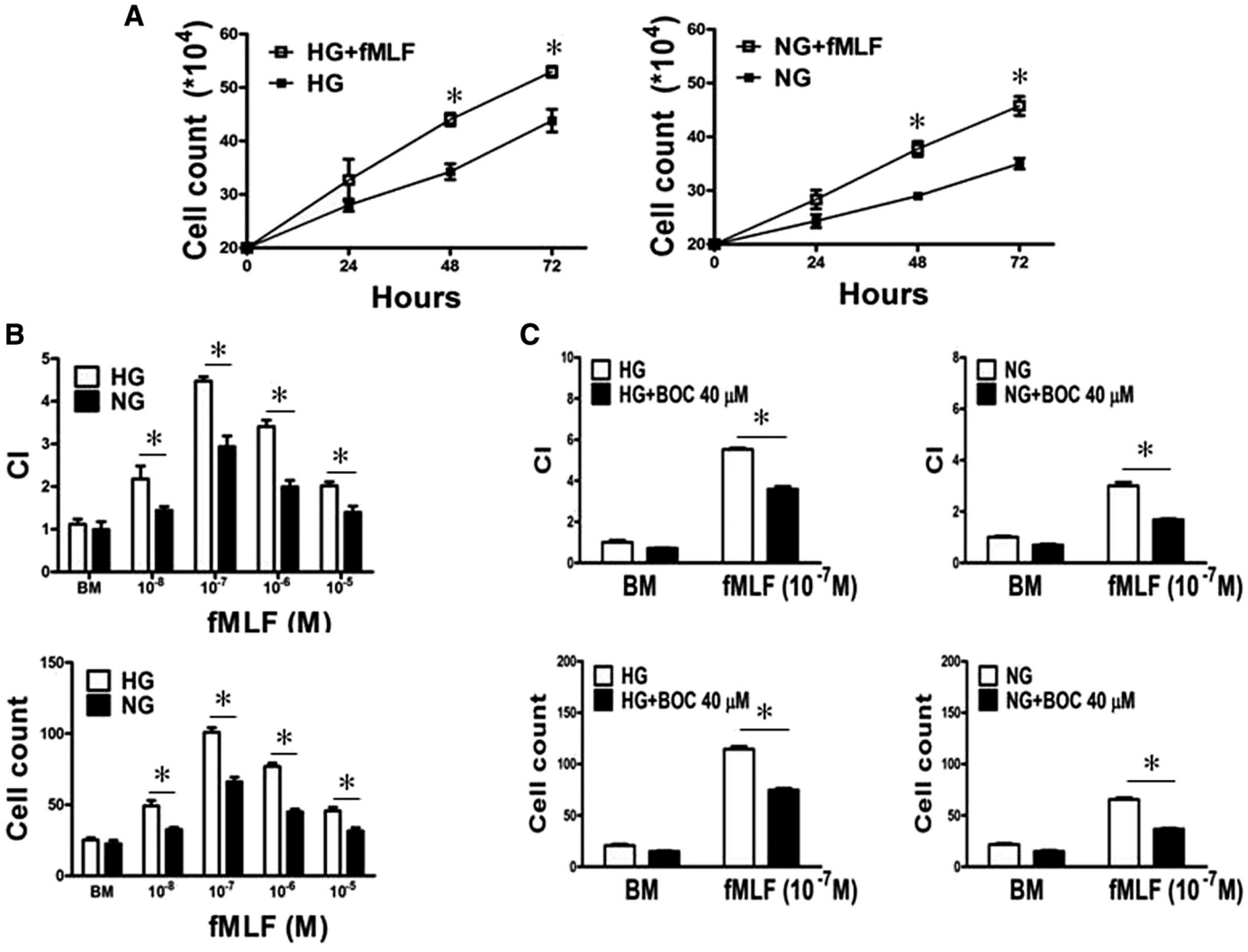

Figure 3. HG enhances the function of FPR1 expressed by U87 cellsA. U87 cell proliferation examined in the absence or presence of the FPR1 agonist fMLF (10^{-7} M) in HG or NG culture for 24, 48 and 72 h. *$P < .05$, indicates significantly increased growth of U87 cells under both HG and NG culture when treated with fMLF. **B.** Migration of U87 cells treated with HG or NG in response to fMLF. *$P < .05$, indicates significantly increased fMLF-induced migration of U87 cells under HG compared with cells in NG. Cell chemotaxis was measured by 48 well chemotaxis chambers. Results are expressed as chemotaxis index (CI) and numbers of migrated cells in response to chemoattractants. **C.** Inhibition of fMLF (10^{-7} M) induced chemotaxis of U87 cells by the FPR1 antagonist BOC-MLF (40 μM). *$P < .05$, indicates significant inhibition of fMLF induced chemotaxis of HG cultured U87 cells by BOC-MLF.

with Prism Version 5.0 software (GraphPad). A two-tailed Student's *t* test or ANOVA was used for evaluating statistical significance of the difference between testing and control groups. $P < .05$ was considered as statistically significant.

Results

HG Promotes U87 Cell Proliferation

We first cultured U87 cells in medium containing NG (5.5 mM glucose) or HG (25 mM glucose) corresponding to normal physiological or diabetic levels in human blood, respectively [14]. U87 cells cultured in HG (U87-HG) increased proliferation compared with cells in NG (U87-NG) (Figure 1, *A* and *B*). U87-HG cells also showed increased sphere formation ability, i.e. the clonogenicity, an indicator of longer-term cell survival and increased tumorigenesis of the tumor cells (Figure 1*C*). This was accompanied by a marked increase in anti-apoptotic Bcl-2 and Mcl-1 proteins in U87-HG cells (Figure 1*D*). Thus, HG provides favorable growth conditions for U87 cells.

HG Up-Regulates the Expression of FPR1 and EGFR by U87 Cells

Since FPR1 and EGFR co-operate to increase the malignant behavior of GBM cells [10,11], we investigated the capacity of HG to regulate these receptors in U87 cells. Figure 2, *A–C*, show that FPR1 mRNA and protein in U87 cells were significantly increased after 24 h culture in HG. The effect of HG was mediated through an NF-κB dependent pathway shown by increased NF-κB phosphorylation (Figure 2, *D* and *E*) in U87-HG cells, which was attenuated by an NF-κB inhibitor, BAY 11–7082 (Figure 2*F*). HG also significantly up-regulated EGFR protein expression in U87 cells (Supplemental Figure 1), suggesting the capacity of HG to promote the expression of both chemotaxis and growth factor receptors by GBM cells.

HG Enhances the Function of FPR1 and EGFR in U87 Cells

FPR1 ligand fMLF enhanced U87 cell proliferation and chemotaxis in both HG and NG media, with more pronounced effect on cells in HG (Figure 3, *A* and *B* and Supplemental Figure 2*A*). Both U87-HG cell and U87-NG cell chemotaxis induced by fMLF was diminished by the FPR1 antagonist BOC-MLF (Figure 3*C* and Supplemental Figure 2*B*), confirming the involvement of FPR1. U87-HG cells additionally showed increased proliferation and chemotaxis in responses to EGF, which was abolished by the EGFR inhibitor AG1478 (Supplemental Figure 3).

HG Accelerates U87 Cell Monolayer Wound Closure

The increased motility of U87-HG cells was supported by scratch-wound healing model, in which HG stimulated a more rapid closure of the wound on GBM cell monolayer. Presence of fMLF or EGF further accelerated the healing of the wound (Figure 4*A*, and

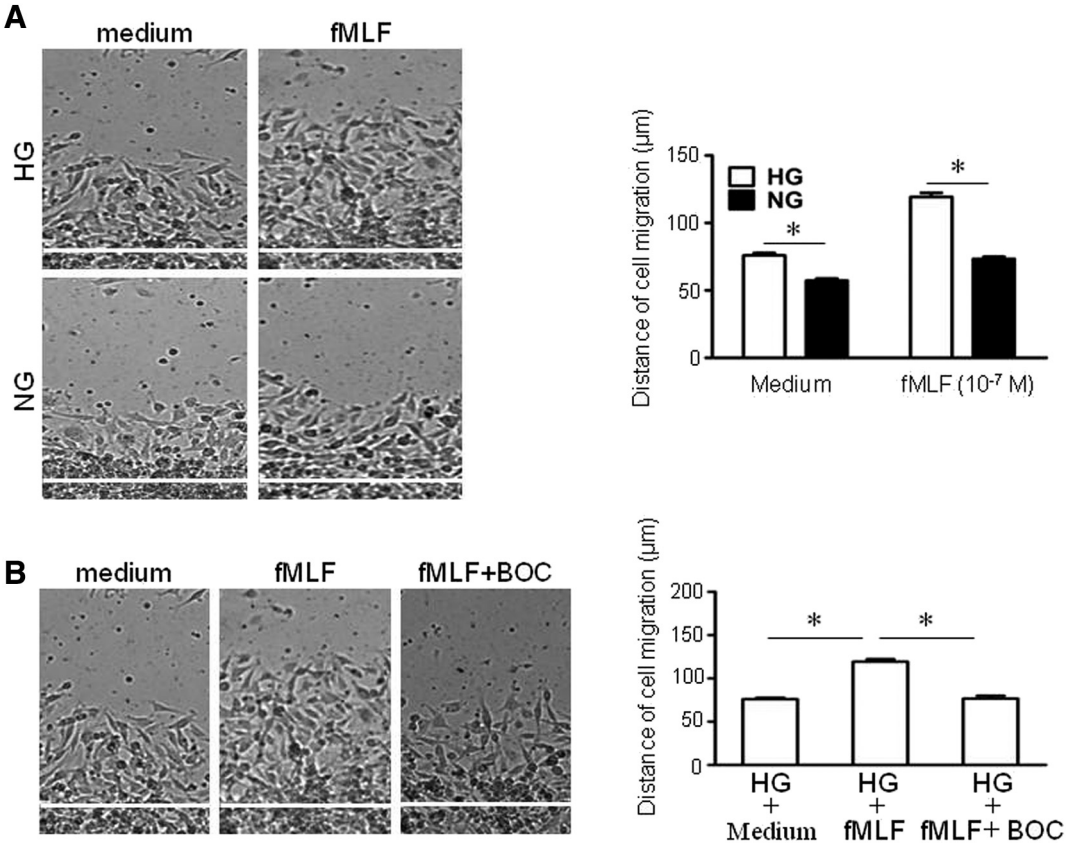

Figure 4. HG accelerates fMLF-induced wound closure by U87 cells. Increased rate of closure of scratch wound on the monolayer of U87 cells in HG or NG culture when treated with fMLF (10^{-7} M) **A.** Wound closure measured at 8 h. Quantitation of cell migration based on results shown in the left panel. *$P < .05$, indicates significantly increased rate of wound closure shown by U87 cells cultured in HG compared with cells in NG. **B.** Inhibition of U87 cell wound closure by the FPR1 antagonist BOC-MLF (40 μM) in HG for 8 h. Quantification of cell migration is based on results shown in the left panel. *$P < .05$, indicates significant inhibition by BOC-MLF of fMLF induced wound closure by U87 cells cultured in HG.

Supplemental Figure 4*A*), which was attenuated by addition of BOC-MLF or AG 1478, the inhibitors of FPR1 (Figure 4*B*) or EGFR, respectively (Supplemental Figure 4*B*). Thus, HG enhances GBM cell wound healing in response to both FPR1 and EGFR agonists by up-regulating their receptors.

U87-HG Cells Produce Increased VEGF in Response to FPR1 and EGFR Agonists

Since VEGF is an important mediator of tumor angiogenesis, we measured VEGF production by U87 cells. HG alone increased the VEGF mRNA in U87 cells with measurable production of VEGF protein, both of which were further enhanced by fMLF treatment (Figure 5, *A* and *B*). Similar results were observed in U87-HG cells stimulated by EGF (Figure 5*C*). Thus, HG promotes the angiogenic capacity of U87 cells through FPR1 and EGFR activation.

HG Enhances MAPK-Signaling in U87 Cells in Response to FPR1 and EGFR Ligands

Since MAPKs regulate malignant signals in cancer cells, we investigated the effect of HG on MAPK activation in U87 cells. U87-HG cells showed increased sensitivity to fMLF by higher levels and more rapid phosphorylation of p38 and ERK1/2, which was inhibited by the FPR1 antagonist CsH (Cyclosporin H) (Figure 6, *A–D*). U87-HG cells also showed increased phosphorylation of NF-κB in response to fMLF (Figure 6*E*). Additionally, EGF stimulated increased phosphorylation of p38 and ERK1/2 in U87-HG cells, which was attenuated by EGFR antagonist AG 1478 (Supplemental Figure 5, *A–D*). Thus, HG amplifies U87 cell responsiveness to FPR1 and EGFR to activate vital signaling pathways.

Diabetes Promotes the Rapid Growth of Xenograft Tumors Formed by U87 Cells

We then validated the effect of diabetes on the growth of xenograft GBM in nude mice. Figure 7*A* shows more rapid growth of tumors formed by U87 cells in diabetic mice with larger tumor size, increased number of Ki67$^+$ proliferating tumor cells, (Figure 7*B*) and invasion into surrounding connective tissues (Figure 7*C*). In contrast, tumors formed in control nude mice were significantly smaller and well encapsulated. We previously reported that xenograft tumors formed by GBM cells were well vascularized [15]. Here we show that xenograft tumors formed in diabetic nude mice contained increased number of EC-like cells as compared with those in non-diabetic mice (Figure 7*D*). These tumors also expressed higher levels of vimentin, a marker for poorly differentiated astroglial cells [16], but reduced glial fibrillary acidic protein (GFAP), a glial differentiation marker [16] (Supplemental Figure 6, *A* and *B*). Therefore, diabetes promotes more rapid growth and invasion of xenograft tumors with an increased malignant phenotype.

Discussion

Growing evidence indicates that glucose metabolism plays an important role in the development and growth of GBM [3,4,17]. Malignant cells are highly dependent on glycolysis for ATP generation, known as the Warburg effect [18] in which withdrawal of glucose resulted in apoptosis of GBM cell lines but not normal human astrocytes [19]. In animal models, ketogenic diet and 2-deoxy-D-glucose administration sensitize GBM to radio- or chemo-therapy leading to prolonged animal survival [20,21]. Patients with type 2 diabetes concomitantly suffer from hyperinsulinemia, which facilitates tumor growth by stimulating insulin-like growth factor (IGF) receptor signaling cascade in tumor cells [22,23] to promote GBM cell proliferation and migration [24]. Our study confirms the capacity of HG to increase the malignant behavior of GBM cells, and more importantly, HG enhanced the expression and function of the chemoattractant receptor FPR1 and EGFR in GBM cells that control tumor cell migration and growth in response to ligands that are present in the tumor microenvironment [10,11]. Furthermore, the

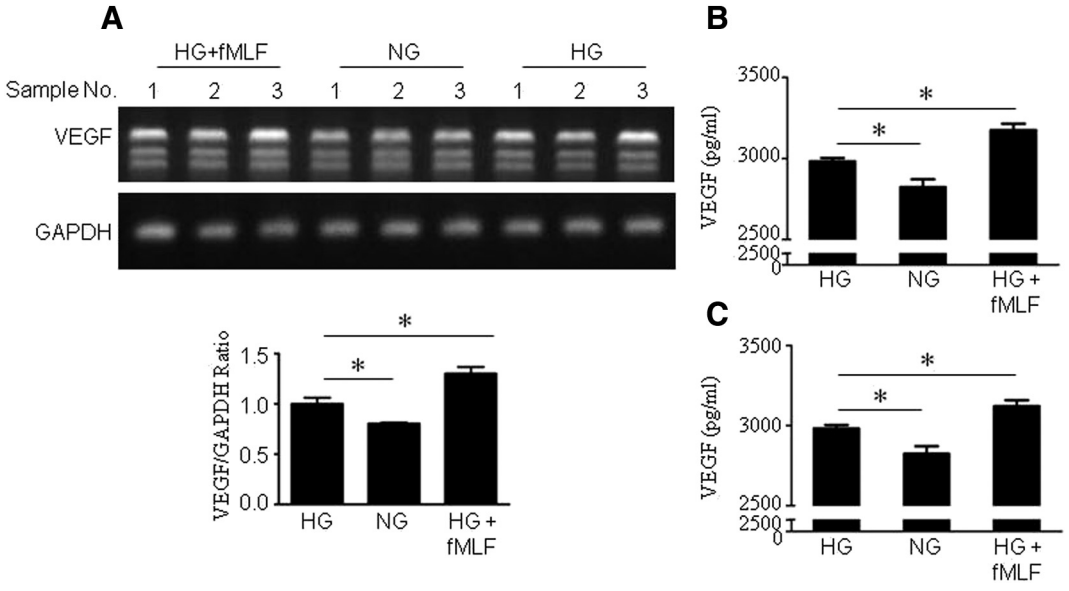

Figure 5. Increased production of VEGF by U87 cells cultured in HG and further enhancement by the presence of FPR1 agonists. U87 cells were cultured in HG or NG with the presence or absence of fMLF or EGF for 24 h. **A.** VEGF mRNA was measured by RT-PCR. **B.** VEGF protein level in the supernatants measured by ELISA. *$P < .05$, indicates significantly increased VEGF mRNA and protein expression by U87 cells in HG compared with cells in NG culture. Further increased VEGF production by U87-HG treated with fMLF (10^{-7} M). **C.** VEGF protein level in the supernatants measured by ELISA. *$P < .05$, indicates significantly increased VEGF protein in U87 cells under HG compared with cells in NG, EGF further increased VEGF productin by U87-HG treated with EGF (10 ng/ml).

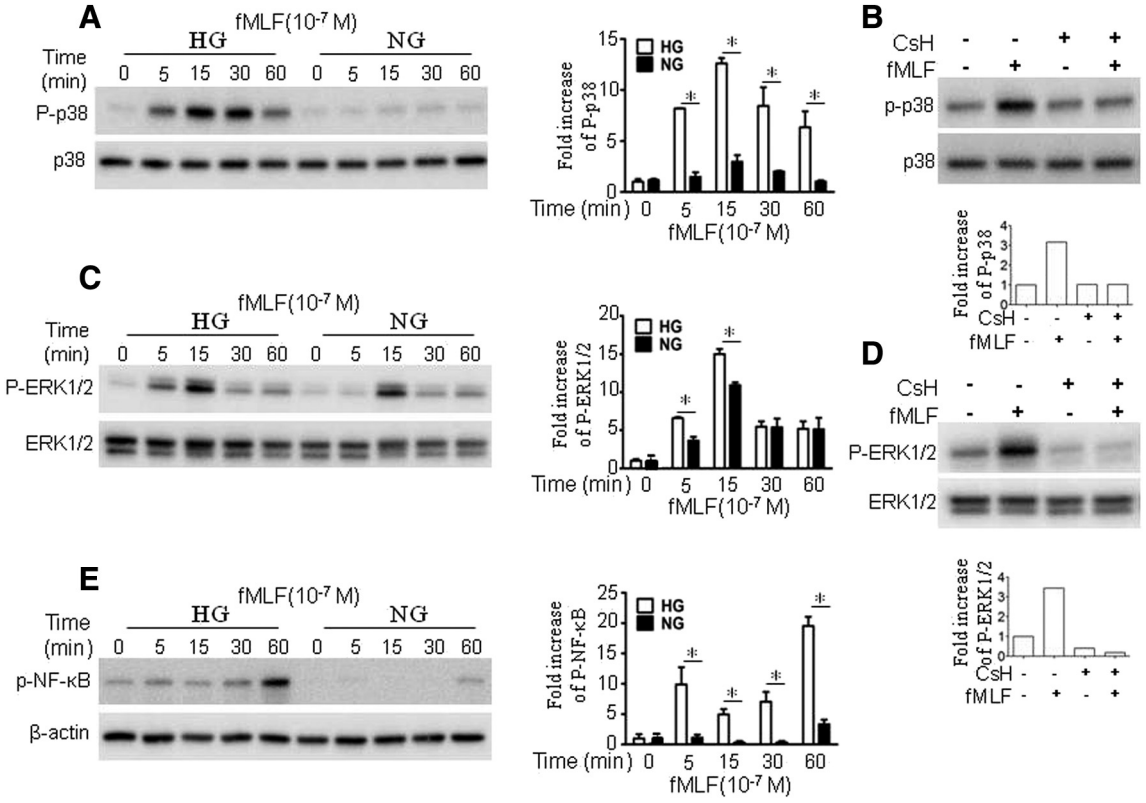

Figure 6. Activation of MAPKs in U87 cells. Western blotting was performed to examine the phosphorylation of p38 and ERK1/2 MAPKs in U87 cells. **A.** p38 phosphorylation induced by fMLF (10^{-7} M) at indicated time in U87 cells cultured with HG or NG. Densitometry quantification of P-p38 was normalized against total p38. *$P < .05$, indicates significantly increased p38 phosphorylation induced by fMLF in U87 cells cultured in HG compared with cells in NG. **B.** p38 phosphorylation in U87 cells in HG inhibited by the FPR1 antagonist, CsH. **C.** ERK1/2 phosphorylation induced by fMLF (10^{-7} M) at indicated time in U87 cells cultured with HG or NG. Densitometry quantification of P-ERK1/2 normalized against total ERK1/2. *$P < .05$, indicates significantly increased ERK1/2 phosphorylation induced by fMLF in U87 cells cultured in HG compared with cells in NG. **D.** ERK1/2 phosphorylation in HG in the presence of fMLF was inhibited by the FPR1 antagonist, CsH. **E.** NF-κB phosphorylation induced by fMLF (10^{-7} M) at indicated times in U87 cells cultured with HG or NG. Densitometry quantification of P-NF-κB normalized against β-actin. *$P < .05$, indicates significantly increased ERK1/2 phosphorylation induced by fMLF in U87 cells cultured in HG compared with cells in NG.

xenograft model validated the notion that GBM tumors grow more rapidly in diabetic nude mice, with increased invasiveness and vascularization. The pathophysiological significance of FPR1 expression by GBM cells was also evidence by the capacity of FPR1 to recognize an endogenous agonist Annexin 1 (Anx A1), which was released by necrotic GBM cells to activate live tumor cells. This was considered as an important autocrine and/or paracrine loop for FPR1 on GBM cells to sense microenvironmental stimulants for tumor progression [25].

FPR1 is a GPCR originally reported to mediate leukocyte chemotaxis and activation in response to bacterial formylated chemotactic peptides. Agonist binding to FPR1 elicits a signal transduction cascade activating mitogen-activated protein kinases (MAPKs) and NF-κB [10,26,27]. In human glioma, FPR1 was found to be selectively expressed by more highly malignant GBM cells [10]. The contribution of FPR1 to GBM progression was further detected in studies showing that small interference RNA targeting of FPR1 markedly reduced the tumorigenic capacity of GBM cells in nude mice. Implanted CD133/Nestin+ glioma stem-like cells expressing FPR1 formed more rapidly growing tumors and produced higher levels of angiogenic factors as a consequence of FPR1 activation [28]. Moreover, targeting FPR1 with a specific antagonist reduced glioma cell motility and prolonged the survival of tumor-bearing mice [29]. Thus, FPR1 appears to possess oncogenic properties in glioma. It is worth noting that U87 cells also express a low level of the FPR1 variant FPR2 transcripts. However, the cells failed to respond to any FPR2 agonists tested suggesting negligible involvement of FPR2 in promoting the malignant behavior of U87 cells.

MAPKs participate in diverse patho-physiological processes [30]. MAPKs are activated in GBM cells by FPR1 and EGFR ligands [10,31], and the effects are enhanced by HG as shown in this study. In STZ-induced diabetic rats, the levels of p-p38 and p-ERK1/2 are elevated in the heart, causing cardiomyopathy [32]. HG media or hyperglycemic sera from type 2 diabetic patients impair the differentiation of dendritic cells (DCs), resulting in immune dysfunction, which is attributable to activation of p38 MAPK pathways [33]. Thus, MAPK signaling is likely involved in the effect of HG on exacerbated GBM cell malignancy. In fact, HG increased the sensitivity of GBM cells to stimulation by FPR1 and EGFR ligands, as evidenced by higher level and more rapid phosphorylation of p38 and ERK1/2, associated with increased GBM cell motility and growth.

EGFR as a receptor tyrosine is upregulated in many cancers and, by responding to multiple endogenous agonists, confers unfavorable

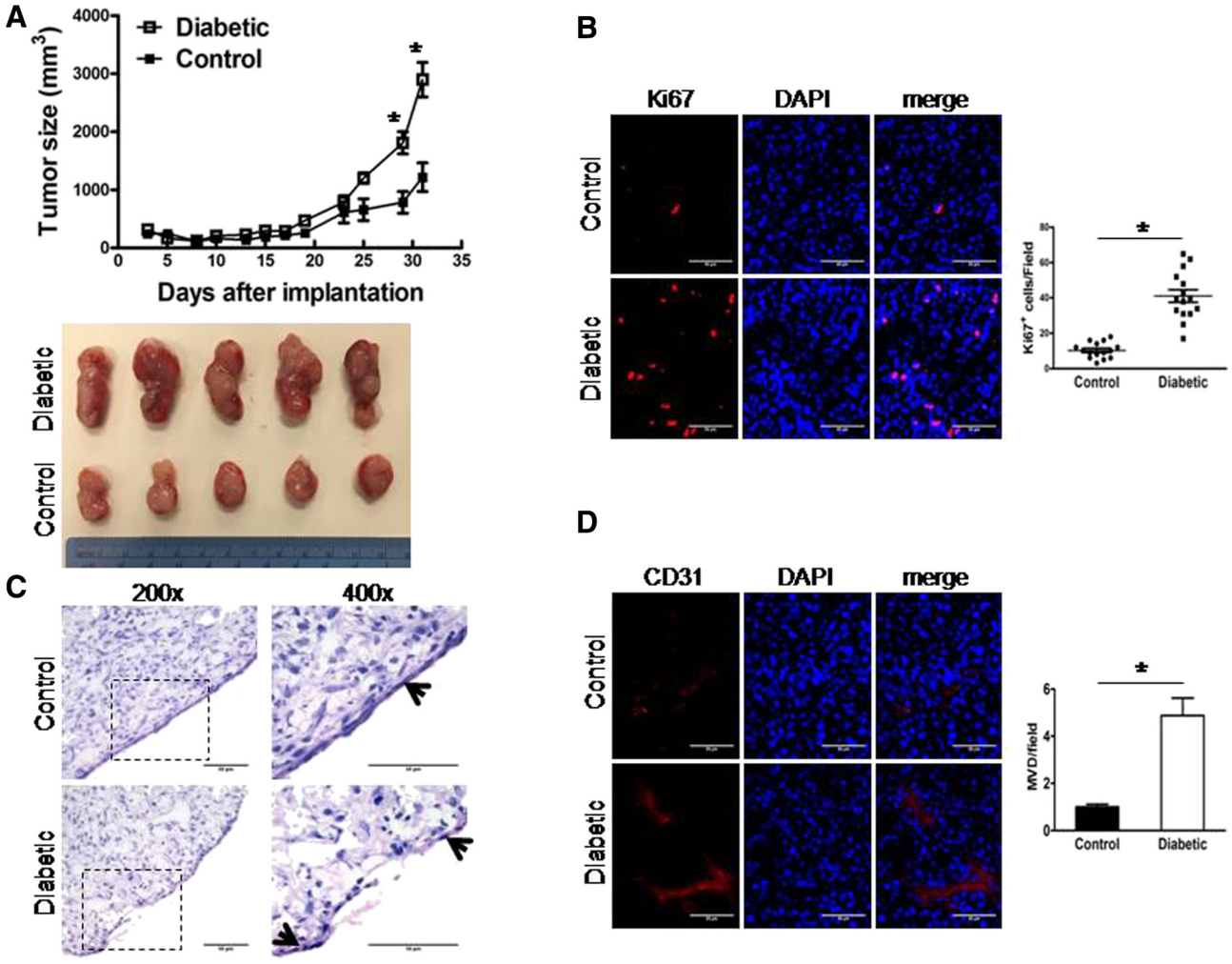

Figure 7. HG promotes the malignant behavior of xenograft tumors formed by U87 cells. Nude mice were injected intraperitoneally with SZT (40 mg/kg) for 5 consecutive days for 2 rounds to establish diabetes mellitus. Mice with stable blood glucose levels above 200 mg/dl are considered as diabetic. **A.** Tumors formed by GBM cells injected subcutaneously into right flanks of normal and diabetic nude mice. Mice were examined for tumor formation at indicated time points. Tumor size was measured at different times after inoculation. *$P < .05$, indicates more rapid growth of human GBM xenograft tumors in diabetic mice. **B.** Ki67 staining for xenograft tumors at day 31 after inoculation. Red: Ki67, Blue: DAPI, Scale bar: 50 μm. Right panel showing quantification of Ki67$^+$ cells in xenograft tumors at day 31 after inoculation in each mouse at three different areas under high power fields (×200), 5 mice per group. *$P < .05$, indicates more rapid growth of human GBM xenograft tumors in diabetic mice. **C.** Histology of tumors formed by U87 cells at day 31. Black arrow: tumor capsule. Scale bar: 50 μm. **D.** Vascular endothelial cells (ECs) detected with anti-mouse CD31 antibodies in tumors formed by U87 cells. Red: CD31, Blue: DAPI, Scale bar: 50 μm. Right panel showed quantification of CD31$^+$ cells in xenograft tumors at day 31 after inoculation in three different areas under high power fields (×200), 5 mice per group. *$P < .05$, indicates increased angiogenesis of human GBM xenograft tumors in diabetic mice.

prognosis to patients [34,35]. EGFR ligands are secreted by glioma as well as stromal cells such as microglia and reactive astrocytes [36]. EGFR overexpression and/or gene mutation are frequently observed in primary GBM, which is associated with poorer patient survival [37]. EGFR is also transactivated by FPR1 agonists in GBM cells and the 2 receptors cooperated to enhance tumor cell survival, invasiveness, and angiogenic factor production [11]. This study further indicates the capacity of HG to increase the malignancy of GBM cells by favoring their responses to both migratory and proliferative stimulants.

In conclusion, HG provides GBM cells with substrates for more rapid growth with enhanced chemotaxis, and production of VEGF mediated by both chemoattractant and growth factor receptors FPR1 and EGFR. Thus, controlling hyperglycemia and overexpression of FPR1 and EGFR may constitute novel strategies to reversing the detrimental effect of diabetes on GBM progression.

Acknowledgements

This project has been funded in part by Federal funds from the National Cancer Institute (NCI), National Institutes of Health (NIH), under Contract No. HSN261200800001E, and by the Intramural Research Programs of the NCI and the NIAID, NIH. ZB was also supported in part by a fund from Shanghai Jiaotong University YG2016QN63.

The authors thank Dr. Joost J. Oppenheim for critically reviewing the manuscript; Mr. Timothy Back for assistance in animal experiments. The secretarial assistance by Ms. Cheri A. Rhoderick is appreciated.

Conflicts of interest

The authors declare no conflicts of interest.

Appendix A. Supplementary data

Supplementary data to this article can be found online at https://doi.org/10.1016/j.tranon.2019.04.016.

References

[1] Ostrom QT, Gittleman H, Fulop J, Liu M, Blanda R, Kromer C, Wolinsky Y, Kruchko C, and Barnholtz-Sloan JS (2015). CBTRUS Statistical Report: Primary brain and central nervous system tumors diagnosed in the United States in 2008-2012. *Neuro Oncol* **17**(Suppl 4), iv1–iv62.

[2] Braganza MZ, Kitahara CM, Berrington de Gonzalez A, Inskip PD, Johnson KJ, and Rajaraman P (2012). Ionizing radiation and the risk of brain and central nervous system tumors: a systematic review. *Neuro Oncol* **14**, 1316–1324.

[3] Chaichana KL, McGirt MJ, Woodworth GF, Datoo G, Tamargo RJ, Weingart J, Olivi A, Brem H, and Quinones-Hinojosa A (2010). Persistent outpatient hyperglycemia is independently associated with survival, recurrence and malignant degeneration following surgery for hemispheric low grade gliomas. *Neurol Res* **32**, 442–448.

[4] Chambless LB, Parker SL, Hassam-Malani L, McGirt MJ, and Thompson RC (2012). Type 2 diabetes mellitus and obesity are independent risk factors for poor outcome in patients with high-grade glioma. *J Neurooncol* **106**, 383–389.

[5] Ogurtsova K, da Rocha Fernandes JD, Huang Y, Linnenkamp U, Guariguata L, Cho NH, Cavan D, Shaw JE, and Makaroff LE (2017). IDF Diabetes Atlas: Global estimates for the prevalence of diabetes for 2015 and 2040. *Diabetes Res Clin Pract* **128**, 40–50.

[6] Scappaticcio L, Maiorino MI, Bellastella G, Giugliano D, and Esposito K (2017). Insights into the relationships between diabetes, prediabetes, and cancer. *Endocrine* **56**, 231–239.

[7] Giovannucci E, Harlan DM, Archer MC, Bergenstal RM, Gapstur SM, Habel LA, Pollak M, Regensteiner JG, and Yee D (2010). Diabetes and cancer: a consensus report. *Diabetes Care* **33**, 1674–1685.

[8] Vasconcelos-Dos-Santos A, Loponte HF, Mantuano NR, Oliveira IA, de Paula IF, Teixeira LK, de-Freitas-Junior JC, Gondim KC, Heise N, and Mohana-Borges R, et al (2017). Hyperglycemia exacerbates colon cancer malignancy through hexosamine biosynthetic pathway. *Oncogene* **6**, e306.

[9] Yu Y, Bao Z, Wang X, Gong W, Chen H, Guan H, Le Y, Su S, Chen K, and Wang JM (2017). The G-protein-coupled chemoattractant receptor Fpr2 exacerbates high glucose-mediated proinflammatory responses of Muller glial cells. *Front Immunol* **8**, 1852.

[10] Zhou Y, Bian X, Le Y, Gong W, Hu J, Zhang X, Wang L, Iribarren P, Salcedo R, and Howard OM, et al (2005). Formylpeptide receptor FPR and the rapid growth of malignant human gliomas. *J Natl Cancer Inst* **97**, 823–835.

[11] Huang J, Hu J, Bian X, Chen K, Gong W, Dunlop NM, Howard OM, and Wang JM (2007). Transactivation of the epidermal growth factor receptor by formylpeptide receptor exacerbates the malignant behavior of human glioblastoma cells. *Cancer Res* **67**, 5906–5913.

[12] Chen K, Zhang L, Huang J, Gong W, Dunlop NM, and Wang JM (2008). Cooperation between NOD2 and Toll-like receptor 2 ligands in the up-regulation of mouse mFPR2, a G-protein-coupled Abeta42 peptide receptor, in microglial cells. *J Leukoc Biol* **83**, 1467–1475.

[13] Xiang Y, Yao X, Chen K, Wang X, Zhou J, Gong W, Yoshimura T, Huang J, Wang R, and Wu Y, et al (2016). The G-protein coupled chemoattractant receptor FPR2 promotes malignant phenotype of human colon cancer cells. *Am J Cancer Res* **6**, 2599–2610.

[14] Leontieva OV, Demidenko ZN, and Blagosklonny MV (2014). Rapamycin reverses insulin resistance (IR) in high-glucose medium without causing IR in normoglycemic medium. *Cell Death Dis* **5**, e1214.

[15] Yao X, Ping Y, Liu Y, Chen K, Yoshimura T, Liu M, Gong W, Chen C, Niu Q, and Guo D, et al (2013). Vascular endothelial growth factor receptor 2 (VEGFR-2) plays a key role in vasculogenic mimicry formation, neovascularization and tumor initiation by Glioma stem-like cells. *PloS one* **8**e57188.

[16] Bramanti V, Tomassoni D, Avitabile M, Amenta F, and Avola R (2010). Biomarkers of glial cell proliferation and differentiation in culture. *Front Biosci* (2), 558–570.

[17] Tieu MT, Lovblom LE, McNamara MG, Mason W, Laperriere N, Millar BA, Menard C, Kiehl TR, Perkins BA, and Chung C (2015). Impact of glycemia on survival of glioblastoma patients treated with radiation and temozolomide. *J Neurooncol* **124**, 119–126.

[18] Warburg O (1956). On the origin of cancer cells. *Science* **123**, 309–314.

[19] Jelluma N, Yang X, Stokoe D, Evan GI, Dansen TB, and Haas-Kogan DA (2006). Glucose withdrawal induces oxidative stress followed by apoptosis in glioblastoma cells but not in normal human astrocytes. *Molecular cancer research : MCR* **4**, 319–330.

[20] Safdie F, Brandhorst S, Wei M, Wang W, Lee C, Hwang S, Conti PS, Chen TC, and Longo VD (2012). Fasting enhances the response of glioma to chemo- and radiotherapy. *PloS one* **7**e44603.

[21] Boison D (2017). New insights into the mechanisms of the ketogenic diet. *Curr Opin Neurol* **30**, 187–192.

[22] Djiogue S, Nwabo Kamdje AH, Vecchio L, Kipanyula MJ, Farahna M, Aldebasi Y, and Seke Etet PF (2013). Insulin resistance and cancer: the role of insulin and IGFs. *Endocr Relat Cancer* **20**, R1-17.

[23] Weroha SJ and Haluska P (2012). The insulin-like growth factor system in cancer. *Endocrinol Metab Clin North Am* **41**, 335–350 vi.

[24] Schlenska-Lange A, Knupfer H, Lange TJ, Kiess W, and Knupfer M (2008). Cell proliferation and migration in glioblastoma multiforme cell lines are influenced by insulin-like growth factor I in vitro. *Anticancer Res* **28**, 1055–1060.

[25] Yang Y, Liu Y, Yao X, Ping Y, Jiang T, Liu Q, Xu S, Huang J, Mou H, and Gong W, et al (2011). Annexin 1 released by necrotic human glioblastoma cells stimulates tumor cell growth through the formyl peptide receptor 1. *Am J Pathol* **179**, 1504–1512.

[26] Huang J, Chen K, Chen J, Gong W, Dunlop NM, Howard OM, Gao Y, Bian XW, and Wang JM (2010). The G-protein-coupled formylpeptide receptor FPR confers a more invasive phenotype on human glioblastoma cells. *Br J Cancer* **102**, 1052–1060.

[27] Huang J, Chen K, Huang J, Gong W, Dunlop NM, Howard OM, Bian X, Gao Y, and Wang JM (2009). Regulation of the leucocyte chemoattractant receptor FPR in glioblastoma cells by cell differentiation. *Carcinogenesis* **30**, 348–355.

[28] Yao XH, Ping YF, Chen JH, Xu CP, Chen DL, Zhang R, Wang JM, and Bian XW (2008). Glioblastoma stem cells produce vascular endothelial growth factor by activation of a G-protein coupled formylpeptide receptor FPR. *J Pathol* **215**, 369–376.

[29] Boer JC, Domanska UM, Timmer-Bosscha H, Boer IG, de Haas CJ, Joseph JV, Kruyt FA, de Vries EG, den Dunnen WF, and van Strijp JA, et al (2013). Inhibition of formyl peptide receptor in high-grade astrocytoma by CHemotaxis Inhibitory Protein of S. aureus. *Br J Cancer* **108**, 587–596.

[30] Kim EK and Choi EJ (2015). Compromised MAPK signaling in human diseases: an update. *Arch Toxicol* **89**, 867–882.

[31] Liu M, Zhao J, Chen K, Bian X, Wang C, Shi Y, and Wang JM (2012). G protein-coupled receptor FPR1 as a pharmacologic target in inflammation and human glioblastoma. *Int Immunopharmacol* **14**, 283–288.

[32] Soetikno V, Sari FR, Sukumaran V, Lakshmanan AP, Mito S, Harima M, Thandavarayan RA, Suzuki K, Nagata M, and Takagi R, et al (2012). Curcumin prevents diabetic cardiomyopathy in streptozotocin-induced diabetic rats: possible involvement of PKC-MAPK signaling pathway. *European journal of pharmaceutical sciences : official journal of the European Federation for Pharmaceutical Sciences* **47**, 604–614.

[33] Gilardini Montani MS, Granato M, Cuomo L, Valia S, Di Renzo L, D'Orazi G, Faggioni A, and Cirone M (2016). High glucose and hyperglycemic sera from type 2 diabetic patients impair DC differentiation by inducing ROS and activating Wnt/beta-catenin and p38 MAPK. *Biochim Biophys Acta* **1862**, 805–813.

[34] Goffin JR and Zbuk K (2013). Epidermal growth factor receptor: pathway, therapies, and pipeline. *Clin Ther* **35**, 1282–1303.

[35] Normanno N, De Luca A, Bianco C, Strizzi L, Mancino M, Maiello MR, Carotenuto A, De Feo G, Caponigro F, and Salomon DS (2006). Epidermal growth factor receptor (EGFR) signaling in cancer. *Gene* **366**, 2–16.

[36] Hoelzinger DB, Demuth T, and Berens ME (2007). Autocrine factors that sustain glioma invasion and paracrine biology in the brain microenvironment. *J Natl Cancer Inst* **99**, 1583–1593.

[37] Nakada M, Kita D, Teng L, Pyko IV, Watanabe T, Hayashi Y, and Hamada J (2013). Receptor tyrosine kinases: principles and functions in glioma invasion. *Adv Exp Med Biol* **986**, 143–170.